

# Surface-Bound Helical Polyacetaldehyde Chains and Bidentate Acetate Intermediates on Ag{111}

W. S. Sim, P. Gardner,<sup>†</sup> and D. A. King\*

Contribution from the Department of Chemistry, University of Cambridge, Lensfield Road, Cambridge CB2 1EW, UK

Received February 29, 1996<sup>⊗</sup>

**Abstract:** The interaction of acetic acid and acetaldehyde with preoxidized Ag{111} has been studied using reflection absorption infrared spectroscopy. A bidentate bridging acetate species which shows no coverage-dependent orientation can be formed either by direct deprotonation of acetic acid by surface atomic O at 240 K or via O-induced polymerization of acetaldehyde at 140 K, followed by decomposition of the polyacetaldehyde intermediate into ethane-1,1-dioxy fragments that dehydrogenate at 220 K. A symmetry analysis reveals that the vibrational spectra of polyacetaldehyde and paraformaldehyde on many metal surfaces can be best interpreted in terms of helical chain structures bound to the surface by skeletal O atoms located along various points of the polymer backbones.

## 1. Introduction

Acetic acid and acetaldehyde represent the simplest homologues of the carboxylic acid and aldehyde series respectively that contain an alkyl fragment linked to the main functional group. The incorporated methyl group is expected to influence their bonding and reactivity either through steric or electronic effects. Both molecules are also important oxidation products in heterogeneous catalytic processes, and as such their adsorption and reactivity on metal surfaces has received considerable attention.<sup>1,2</sup>

Surface-bound acetate is generally produced when acetic acid is deprotonated by clean or preoxidized transition metal surfaces. It is a fairly stable species, and persists up to 600 K on Ag{110}<sup>3,4</sup> and Cu{110},<sup>5</sup> above which it breaks down into CO, CO<sub>2</sub>, H<sub>2</sub>, H<sub>2</sub>O, and ketene. Dehydrogenation of acetate to give H<sub>2</sub> and CO<sub>2</sub>, and in some cases CO and surface C as well, has been reported on Ni{111},<sup>6</sup> Ni{110},<sup>7</sup> Ni{100},<sup>8</sup> Pt{111},<sup>9</sup> Pd{111},<sup>10</sup> Pd{110},<sup>11</sup> Rh{111},<sup>12,13</sup> and Rh{110}.<sup>14</sup> In some cases autocatalytic decomposition has been observed,<sup>7,11–14</sup> and the involvement of an acetic anhydride intermediate has also been proposed.<sup>7,15</sup>

The adsorption behavior of acetaldehyde on metal surfaces is more complex and involves a wider spectrum of intermediate surface species. Coordination via the O lone pair orbitals results in the weakly bound  $\eta^1(\text{O})$  state, which typically desorbs without reaction. This species has been observed at low temperatures (<200 K) on Pd{111},<sup>16</sup> Ru{001},<sup>17</sup> and Cu{111}.<sup>18</sup> In the

$\eta^2(\text{C,O})$  state, interaction occurs through the C=O  $\pi$  orbitals, and the stronger bonding to the surface allows competitive decomposition processes to take place. Investigations of this species on Pd{111},<sup>16</sup> Ru{001},<sup>17</sup> Pt(S){6{111} × {100}},<sup>19</sup> and Ni{100}<sup>20</sup> indicate that it breaks down into a mixture of CO, H<sub>2</sub>, and hydrocarbon fragments. Another possibility is surface-induced polymerization of acetaldehyde, which has been reported to occur on Ru{001}<sup>17</sup> and O-covered Cu{111}.<sup>18</sup> Polymerization also occurs within condensed multilayers of acetaldehyde on Ru{001}<sup>17</sup> and Rh{111},<sup>21</sup> as well as several higher aldehydes on Rh{111}.<sup>22</sup> The surface-bound polymeric species acts as the precursor to the formation of  $\eta^2(\text{C,O})$ -acetaldehyde and acetate.

Acetaldehyde and acetate have been implicated as reaction intermediates in the total combustion pathway during the epoxidation of ethylene.<sup>23</sup> Model thermal desorption studies under ultrahigh vacuum (UHV) on preoxidized Ag{110} suggest that acetaldehyde is oxidized to acetate,<sup>3</sup> which in the presence of an excess of surface O decomposes via a new route to formate, CO<sub>2</sub>, and H<sub>2</sub>O.<sup>4,24</sup> There have been no reported spectroscopic studies of this system on Ag{111}, and the few vibrational spectra on other metal surfaces have been collected at relatively low spectral resolutions. In this paper we describe the use of high resolution reflection absorption infrared spectroscopy (RAIRS) to probe the low-temperature oxidation of acetaldehyde and acetic acid on Ag{111} and present evidence for the formation of surface polyacetaldehyde and acetate species.

## 2. Experimental Section

The UHV system used for these experiments, based around a Mattson Cygnus 100 Fourier-transform spectrometer, has been described in detail elsewhere.<sup>25</sup> RAIR spectra were obtained by the coaddition of 500

<sup>†</sup> Current address: Department of Chemistry, UMIST, P.O. Box 88, Manchester M60 1QD, UK.

<sup>⊗</sup> Abstract published in *Advance ACS Abstracts*, October 1, 1996.

- (1) Madix, R. J. *Adv. Catal.* **1980**, *29*, 1.
- (2) Friend, C. M.; Xu, X. *Annu. Rev. Phys. Chem.* **1991**, *42*, 251.
- (3) Barteau, M. A.; Bowker, M.; Madix, R. J. *J. Catal.* **1981**, *67*, 118.
- (4) Sault, A. G.; Madix, R. J. *Surf. Sci.* **1986**, *172*, 598.
- (5) Bowker, M.; Madix, R. J. *Appl. Surf. Sci.* **1981**, *8*, 299.
- (6) Schoofs, G. R.; Benziger, J. B. *Surf. Sci.* **1984**, *143*, 359.
- (7) Madix, R. J.; Falconer, J. L.; Suszko, A. M. *Surf. Sci.* **1976**, *54*, 6.
- (8) Scharpf, E. W.; Benziger, J. B. *J. Phys. Chem.* **1987**, *91*, 5531.
- (9) Avery, N. R. *J. Vac. Sci. Technol.* **1982**, *20*, 592.
- (10) Davis, J. L.; Barteau, M. A. *Surf. Sci.* **1991**, *256*, 50.
- (11) Aas, N.; Bowker, M. *J. Chem. Soc., Faraday Trans.* **1993**, *89*, 1249.
- (12) Li, Y. X.; Bowker, M. *Surf. Sci.* **1993**, *285*, 219.
- (13) Hoogers, G.; Papageorgopoulos, D. C.; Ge, Q.; King, D. A. *Surf. Sci.* **1995**, *340*, 23.
- (14) Li, Y. X.; Bowker, M. *J. Catal.* **1993**, *142*, 630.
- (15) Erley, W.; Chen, J. G.; Sander, D. *J. Vac. Sci. Technol. A* **1990**, *8*, 976.

- (16) Davis, J. L.; Barteau, M. A. *J. Am. Chem. Soc.* **1989**, *111*, 1782.
- (17) Henderson, M. A.; Zhou, Y.; White, J. M. *J. Am. Chem. Soc.* **1989**, *111*, 1185.
- (18) Lamont, C. L. A.; Stenzel, W.; Conrad, H.; Bradshaw, A. M. *J. Electron Spectrosc. Rel. Phenom.* **1993**, *64–65*, 287.
- (19) McCabe, R. W.; Dimaggio, C. L.; Madix, R. J. *J. Phys. Chem.* **1985**, *89*, 854.
- (20) Madix, R. J.; Yamada, T.; Johnson, S. W. *Appl. Surf. Sci.* **1984**, *19*, 43.
- (21) Houtman, C. J.; Barteau, M. A. *J. Catal.* **1991**, *130*, 528.
- (22) Brown, N. F.; Barteau, M. A. *J. Phys. Chem.* **1996**, *100*, 2269.
- (23) Grant, R. B.; Lambert, R. M. *J. Catal.* **1985**, *93*, 92.
- (24) Sault, A. G.; Madix, R. J. *J. Phys. Chem.* **1986**, *90*, 4723.

**Table 1.** Vibrational Frequencies and Mode Assignments for CH<sub>3</sub>COO and CD<sub>3</sub>COO

assignment	CH <sub>3</sub> COO <sup>-</sup> aq solution <sup>a</sup> (cm <sup>-1</sup> ) <sup>27</sup>	CH <sub>3</sub> COO Cu{100} <sup>b</sup> (cm <sup>-1</sup> ) <sup>28</sup>	CH <sub>3</sub> COO Ag{111} <sup>a</sup> (cm <sup>-1</sup> )	CD <sub>3</sub> COO <sup>-</sup> aq solution <sup>a</sup> (cm <sup>-1</sup> ) <sup>27</sup>	CD <sub>3</sub> COO Cu{100} <sup>b</sup> (cm <sup>-1</sup> ) <sup>28</sup>	CD <sub>3</sub> COO Ag{111} <sup>a</sup> (cm <sup>-1</sup> )
$\nu_{\text{as}}(\text{CH}_3)/\nu_{\text{as}}(\text{CD}_3)$	3010			2264		
	2981			2231		
$\nu_{\text{s}}(\text{CH}_3)/\nu_{\text{s}}(\text{CD}_3)$	2935	3000	2933	2111	2218	2162
$\delta_{\text{as}}(\text{CH}_3)/\delta_{\text{as}}(\text{CD}_3)$	1456			1047		
	1429			1031		
$\delta_{\text{s}}(\text{CH}_3)/\delta_{\text{s}}(\text{CD}_3)$	1344		1339	1085		1012
$\nu_{\text{as}}(\text{OCO})$	1556			1545		
$\nu_{\text{s}}(\text{OCO})$	1413	1434	1396	1406	1413	1388
$\rho(\text{CH}_3)/\rho(\text{CD}_3)$	1052			940		
	1020			832		
$\nu(\text{CC})$	926	1041		883	1061	
$\delta(\text{OCO})$	650	677		619	648	
$\rho(\text{OCO})$	621			526		
	471			419		

<sup>a</sup> From infrared spectra. <sup>b</sup> From HREEL spectra.

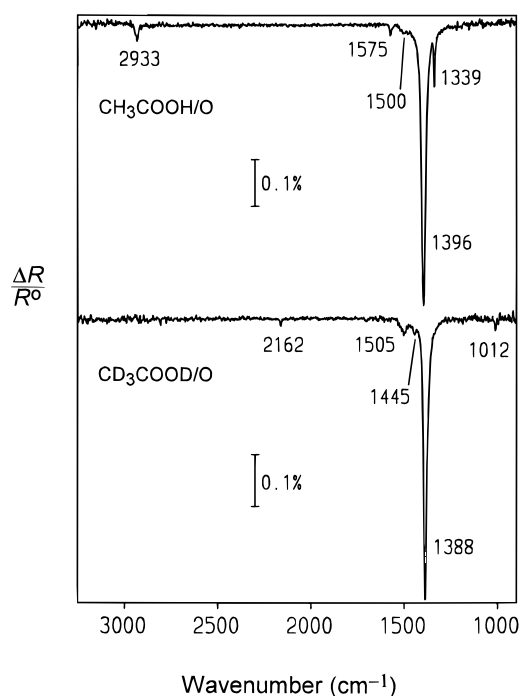


**Figure 1.** RAIR spectra of preoxidized Ag{111} exposed to >1 L of CH<sub>3</sub>COOH and CD<sub>3</sub>COOD at 240 K.

scans at 4-cm<sup>-1</sup> resolution over the spectral range 4000–800 cm<sup>-1</sup> and presented as a ratio against a clean surface spectrum. All RAIR spectra were acquired under isothermal conditions at the temperatures indicated.

The Ag{111} crystal was cleaned by repeated cycles of Ar sputtering at 600 K followed by annealing to 750 K. The atomically adsorbed O-covered surface, characterized by a  $p(4 \times 4)$  LEED pattern, was formed by exposing the clean surface to ~1 mbar of O<sub>2</sub> at 425 K for 5 min, followed by a momentary anneal in vacuum to ~470 K.<sup>26</sup> Acetic acid (CH<sub>3</sub>COOH, Aldrich, 99.99%), acetic-*d*<sub>3</sub> acid-*d* (CD<sub>3</sub>COOD, Aldrich, 99.5% D), acetaldehyde (CH<sub>3</sub>CHO, Aldrich, 99%), and acetaldehyde-*d*<sub>4</sub> (CD<sub>3</sub>CDO, Aldrich, 99% D) were degassed by several freeze–pump–thaw cycles prior to dosing via a leak valve.

### 3. Results

#### 1. RAIR Spectra of Acetate Adsorbed on Ag{111}.

Figure 1 shows the RAIR spectra of preoxidized Ag{111} dosed with saturation exposures (>1 L) of CH<sub>3</sub>COOH and CD<sub>3</sub>COOD at 240 K. They have surprisingly few strong absorption features

and agree well with vibrational spectra of the acetate ion<sup>27</sup> and acetate species observed on other metal surfaces,<sup>9,10,18,28</sup> as summarized in Table 1. Spectra obtained at lower acetic acid exposures were qualitatively similar, and no evidence of adsorbed acetic acid was detected (specifically the strong absorption due to the C=O stretch  $\nu(\text{C}=\text{O})$  expected at ~1700 cm<sup>-1</sup>), confirming that complete deprotonation has occurred under these conditions.

The dominant absorption band due to the symmetric O–C–O stretch  $\nu_{\text{s}}(\text{OCO})$  is observed at 1396 cm<sup>-1</sup> for CH<sub>3</sub>COO and 1388 cm<sup>-1</sup> for CD<sub>3</sub>COO. The corresponding asymmetric O–C–O stretch  $\nu_{\text{as}}(\text{OCO})$ , which usually absorbs as strongly as  $\nu_{\text{s}}(\text{OCO})$  in acetate ligands at 1550–1600 cm<sup>-1</sup>, appears to be infrared inactive in this case. At very high surface coverages, however, small  $\nu_{\text{s}}(\text{OCO})$  and  $\nu_{\text{as}}(\text{OCO})$  bands due to the formation of minority acetate species (possibly associated with defect sites) are detected. These appear at 1500 and 1575 cm<sup>-1</sup> for CH<sub>3</sub>COO and at 1445 and 1505 cm<sup>-1</sup> for CD<sub>3</sub>COO.

Based on their predicted downward shifts on deuteration by a factor of ~0.73, bands at 2933 and 2162 cm<sup>-1</sup> are assigned to the symmetric methyl stretches  $\nu_{\text{s}}(\text{CH}_3)$  and  $\nu_{\text{s}}(\text{CD}_3)$ , respectively, while bands at 1339 and 1012 cm<sup>-1</sup> are attributed to the symmetric methyl deformations  $\delta_{\text{s}}(\text{CH}_3)$  and  $\delta_{\text{s}}(\text{CD}_3)$ , respectively. The remaining vibrational modes that should fall within the detector range are not observed because of their weak or zero dipolar activities. These include the C–C stretch  $\nu(\text{CC})$ , the asymmetric methyl stretches  $\nu_{\text{as}}(\text{CH}_3)$  and  $\nu_{\text{as}}(\text{CD}_3)$ , the asymmetric methyl deformations  $\delta_{\text{as}}(\text{CH}_3)$  and  $\delta_{\text{as}}(\text{CD}_3)$ , and the methyl rocks  $\rho(\text{CH}_3)$  and  $\rho(\text{CD}_3)$ .

#### 2. RAIR Spectra of Acetaldehyde Adsorption and Reaction on Preoxidized Ag{111}.

Figures 2 and 3 shows a series of RAIR spectra obtained by dosing the preoxidized Ag{111} surface with saturation exposures (>5 L) of CH<sub>3</sub>CHO and CD<sub>3</sub>CDO respectively at 140 K, followed by annealing to the temperatures indicated. The absence of the strong  $\nu(\text{C}=\text{O})$  absorption of acetaldehyde at ~1700 cm<sup>-1</sup> and the concurrent appearance of new groups of features at 1070–1230 and ~1400 cm<sup>-1</sup> that are not normally present in the acetaldehyde infrared spectra<sup>29</sup> suggest that reaction has occurred to produce different surface species. From the evolution of the spectra between 140 and 220 K whereby one set of absorption bands grows at the expense of the other, we conclude that at least two surface intermediates are present and that they undergo an irreversible interconversion with increasing temperature.

(25) Raval, R.; Harrison, M. A.; King, D. A.; Caine, G. *J. Vac. Sci. Technol. A* **1991**, *9*, 345.

(26) Sim, W. S.; Gardner, P.; King, D. A. *J. Phys. Chem.* **1995**, *99*, 16002.

(27) Ito, K.; Bernstein, H. J. *Can. J. Chem.* **1956**, *34*, 170.

(28) Sexton, B. A. *Chem. Phys. Lett.* **1979**, *65*, 469.

(29) Hollenstein, H.; Gunthard, H. H. *Spectrochim. Acta A* **1971**, *27*, 2027.

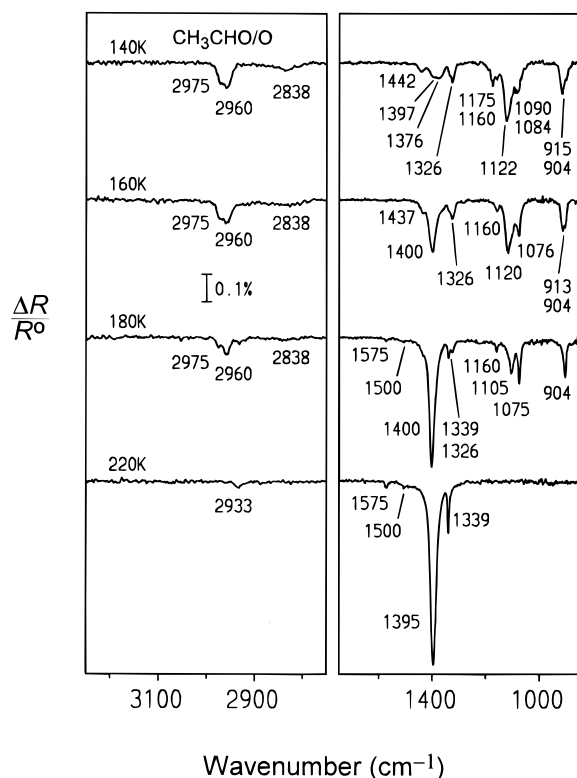


**Figure 2.** RAIR spectra of preoxidized Ag{111} exposed to >5 L of CH<sub>3</sub>CHO at 140 K and then annealed to and maintained at the temperatures indicated.

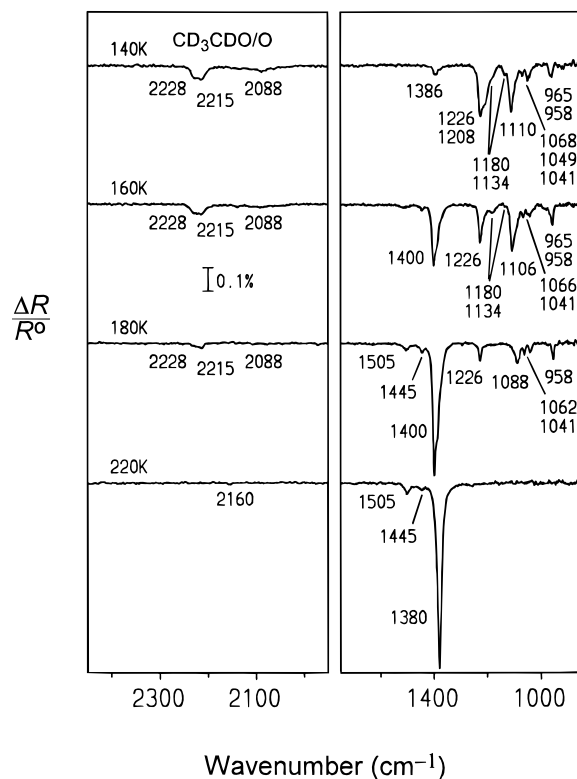


**Figure 3.** RAIR spectra of preoxidized Ag{111} exposed to >5 L of CD<sub>3</sub>CDO at 140 K and then annealed to and maintained at the temperatures indicated.

At 220 K, the spectrum derived from the reaction of each acetaldehyde isotopomer with the adsorbed atomic O is virtually identical to that of the corresponding acetate isotopomer produced by acetic acid deprotonation on Ag{111}, and may be assigned in the same way. By subtracting the acetate features

(essentially the  $\nu_s(\text{OCO})$  band at  $\sim 1400\text{ cm}^{-1}$ ), we are left with the spectra of the remaining surface species at lower temperatures. The series of bands at  $1070\text{--}1230\text{ cm}^{-1}$  is characteristic of compounds containing the O–C–O vicinal diether linkage, and the most likely candidate in the present case is probably some sort of an acetal species ((RO)<sub>2</sub>CHR). It may be in the form of a discrete unit like ethane-1,1-dioxy (CH<sub>3</sub>CHOO), a trimeric ring like paraldehyde ((CH<sub>3</sub>CHO)<sub>3</sub>), or a polymeric chain like polyacetaldehyde ((CH<sub>3</sub>CHO)<sub>x</sub>). Table 2 lists the spectral assignments for a number of relevant systems, and together with further reasons to be discussed below (Section 4.2.), we have interpreted our spectra based on that of crystalline polyacetaldehyde. Several of the bands show distinct splitting into doublets that lose one component on heating, and this will be shown later to be consistent with the polymeric structure.

The doublet at  $2960/2975\text{ cm}^{-1}$  and the band at  $2838\text{ cm}^{-1}$ , which shift on deuteration to  $2215/2228$  and  $2088\text{ cm}^{-1}$ , are attributed to  $\nu_{\text{as}}(\text{CH}_3)/\nu_{\text{as}}(\text{CD}_3)$  and the C–H/C–D stretches  $\nu(\text{CH})/\nu(\text{CD})$ , respectively. For (CH<sub>3</sub>CHO)<sub>x</sub>, we can readily assign  $\delta_{\text{as}}(\text{CH}_3)$  at  $1442\text{ cm}^{-1}$ ,  $\delta_s(\text{CH}_3)$  at  $1376\text{ cm}^{-1}$ , and the in-plane C–H deformation  $\delta(\text{CH})$  at  $1326\text{ cm}^{-1}$ . The  $\nu(\text{CC})$  and  $\rho(\text{CH}_3)$  modes are strongly coupled and are observed at  $1122$  and  $904/915\text{ cm}^{-1}$ , by analogy with the corresponding modes in CH<sub>3</sub>CHO.<sup>29</sup> These are expected to further interact significantly with  $\nu_s(\text{OCO})$  at  $1084/1090\text{ cm}^{-1}$  and  $\nu_{\text{as}}(\text{OCO})$  at  $1160/1175\text{ cm}^{-1}$ . In the case of (CD<sub>3</sub>CDO)<sub>x</sub>, the situation is complicated by the similarity in frequencies of the C–D deformations, C–C stretch, and C–O stretches, which results in intermixing of all these modes. We tentatively assign the weak bands at  $1041/1049$ ,  $1068$ , and  $1134\text{ cm}^{-1}$ , in no particular order, to the coupled modes consisting of  $\delta_{\text{as}}(\text{CD}_3)$ ,  $\delta_s(\text{CD}_3)$ , and the in-plane C–D deformation  $\delta(\text{CD})$ , based on their isotopic shifts by factors of  $0.72\text{--}0.86$ . The doublet at  $958/965\text{ cm}^{-1}$  is due to  $\rho(\text{CD}_3)$ , as seen for CD<sub>3</sub>CDO.<sup>29</sup> The remaining bands at  $1208/1226$ ,  $1180$ , and  $1110\text{ cm}^{-1}$ , by comparison of their frequencies and intensities with those of (CH<sub>3</sub>CHO)<sub>x</sub>, can be attributed to  $\nu_s(\text{OCO})$  (probably pushed upwards by very strong coupling to the C–D deformations),  $\nu_{\text{as}}(\text{OCO})$ , and  $\nu(\text{CC})$ , respectively.

Further heating of the adsorbate layer eventually resulted in the gradual attenuation and eventual disappearance of all the acetate bands at  $\sim 450\text{ K}$  (not shown). No other surface species could be detected spectroscopically during the course of this decomposition process.

#### 4. Discussion

**1. Bonding Configuration of Acetate on Ag{111}.** The application of the metal–surface selection rule in surface vibrational spectroscopy to deduce the bonding geometries of adsorbed species is usually carried out in a rigorous manner by a complete symmetry analysis.<sup>30,31</sup> This treatment yields distinct solutions for high symmetry systems that possess a rotational symmetry axis and mirror planes (i.e. those belonging to the point groups  $C_{2v}$ ,  $C_{3v}$ ,  $C_{4v}$ , and  $C_{6v}$ ) as they each often correspond to only a single possible adsorbate orientation relative to the surface. However, it is much more ambiguous with regard to low-symmetry systems (specifically those with  $C_s$  and  $C_1$  symmetry) where the extra degrees of freedom introduced by the loss of all rotational symmetry elements mean that there are usually many compatible adsorbate configurations associated with each symmetry group. In such cases, provided

(30) Ibach, H.; Mills, D. L. *Electron Energy Loss Spectroscopy and Surface Vibrations*; Academic: London, 1982; p 127.

(31) Richardson, N. V.; Sheppard, N. In *Vibrational Spectroscopy of Molecules on Surfaces*; Yates, J. T., Maday, T. E., Eds.; Plenum: New York, 1987; p 1.

**Table 2.** Vibrational Frequencies and Mode Assignments for  $(\text{CH}_3\text{CHO})_x$  and  $(\text{CD}_3\text{CDO})_x^a$ 

assignment	$\text{CH}_3\text{CHO}$ crystalline <sup>b</sup> ( $\text{cm}^{-1}$ ) <sup>29</sup>	$(\text{CH}_3\text{CHO})_3$ crystalline <sup>b</sup> ( $\text{cm}^{-1}$ ) <sup>39</sup>	$(\text{CH}_3\text{CHO})_x$ crystalline <sup>b</sup> ( $\text{cm}^{-1}$ ) <sup>37</sup>	$(\text{CH}_3\text{CHO})_x \text{Cu}\{111\}^c$ ( $\text{cm}^{-1}$ ) <sup>18</sup>	$(\text{CH}_3\text{CHO})_x \text{Ag}\{111\}^b$ ( $\text{cm}^{-1}$ )	$\text{CD}_3\text{CDO}$ crystalline <sup>b</sup> ( $\text{cm}^{-1}$ ) <sup>29</sup>	$(\text{CD}_3\text{CDO})_x \text{Ag}\{111\}^b$ ( $\text{cm}^{-1}$ )
$\nu_{\text{as}}(\text{CH}_3)/\nu_{\text{as}}(\text{CD}_3)$	3003 2964	2999 2944	2980	2986	2975, 2960	2255 2221	2228, 2215
$\nu_s(\text{CH}_3)/\nu_s(\text{CD}_3)$	2918	2812	2920	2934		2133	
$\nu(\text{CH})/\nu(\text{CD})$	2762	2781	2860		2838	2095	2088
$\nu(\text{C}=\text{O})$	1722					1712	
$\delta_{\text{as}}(\text{CH}_3)/\delta_{\text{as}}(\text{CD}_3)$	1431 1422	1454	1445	1447	1442	1045 1014	1049, 1041
$\delta_s(\text{CH}_3)/\delta_s(\text{CD}_3)$	1347	1371	1380	1380	1376	936	1068
$\delta(\text{CH})/\delta(\text{CD})$	1389	1396, 1344	1400, 1335		1326	1026	1134
$\nu_{\text{as}}(\text{OCO})$		1184, 1174	1187	1174, 1153	1175, 1160		1180
$\nu_s(\text{OCO})$		1105	1085, 1040	1103	1090, 1084		1226, 1208
$\nu(\text{CC})$	1118	1121	1130	1103	1122	1151	1110
$\rho(\text{CH}_3)/\rho(\text{CD}_3)$	889	951	970, 935	947	915, 904	747	965, 958
$\pi(\text{CH})/\pi(\text{CD})$	1102	857	845			948	
$\delta(\text{OCO})$	772	838	810			567	
$\delta(\text{OCO})$		748	620	661			
$\rho(\text{OCO})$		574	490	538			
		527, 474	450				

<sup>a</sup> A brace denotes coupled modes with some reassignment of reported data. <sup>b</sup> From infrared spectra. <sup>c</sup> From HREEL spectra.

**Table 3.** Symmetry Species of the Fundamental Internal Modes of Acetate under the Possible Symmetry Groups of the Surface-Adsorbate Complex and the Polarization States of Their Dynamic Dipole Moments in the Free Acetate Ion (Reference Axes:  $z$  along the C-C Bond,  $y$  Perpendicular to the O-C-O Plane,  $x$  Parallel to the O-C-O Plane)

mode	symmetry group		dynamic dipole moment
	$C_s$	$C_1$	
$\nu_{\text{as}}(\text{CH}_3)$	$A' + A''$	2A	$x + y$
$\nu_s(\text{CH}_3)$	$A'$	A	$z$
$\delta_{\text{as}}(\text{CH}_3)$	$A' + A''$	2A	$x + y$
$\delta_s(\text{CH}_3)$	$A'$	A	$z$
$\nu_{\text{as}}(\text{OCO})$	$A'$	A	$x$
$\nu_s(\text{OCO})$	$A'$	A	$z$
$\nu(\text{CC})$	$A'$	A	$z$
$\rho(\text{CH}_3)$	$A' + A''$	2A	$x + y$
$\delta(\text{OCO})$	$A'$	A	$z$
$\rho(\text{OCO})$	$A' + A''$	2A	$x + y$
$\tau(\text{CH}_3)$	$A''$	A	$y$

that the surface-adsorbate bonding is not too strong, it may still be possible to distinguish between certain bonding geometries by taking into account the directions of the dynamic dipole moments of the normal modes of vibration of the free adsorbate molecule.

The acetate species presents just such a situation. In the free ionic state it possesses  $C_s$  symmetry whereby both the C-O and one of the C-H bonds lie within the mirror plane. By bonding to a solid surface via one (monodentate configuration) or both (bidentate configuration) of its O atoms, acetate can have either  $C_s$  or  $C_1$  symmetry, depending on whether or not its mirror plane is retained. The fifteen internal vibrations of surface-bound acetate have been classified into their symmetry-allowed ( $A$  or  $A'$ ) and symmetry-forbidden ( $A''$ ) irreducible representations under the relevant point groups in Table 3. It is apparent that the symmetry analysis makes no clear distinction between various bonding modes as  $\nu_s(\text{OCO})$  and  $\nu_{\text{as}}(\text{OCO})$ , which often serve as the most useful indicators due to their inherently strong dynamic dipole moments, are both symmetry-allowed transitions under all conditions. If the vibrational modes are described in terms of the polarization state of their dynamic dipole moments with respect to the three orthogonal axes of the acetate fragment instead, as has been done in Table 3, then a much clearer picture emerges. The expected infrared activity of each mode then scales with the normal component of its associated dynamic dipole moment with respect to the surface,

which in turn varies with the orientation of the acetate fragment. Thus, for the C-O stretches, infrared activity of the symmetric mode only would imply symmetrical bidentate bonding, while infrared activity of both modes would indicate monodentate bonding, with  $\nu_{\text{as}}(\text{OCO})$  increasing in intensity at the expense of  $\nu_s(\text{OCO})$  as the degree of tilting in the molecular plane increases.

The RAIR spectrum of acetate (neglecting the minority species) on  $\text{Ag}\{111\}$  only exhibits absorption bands due to  $\nu_s(\text{CH}_3)$ ,  $\delta_s(\text{CH}_3)$ , and  $\nu_s(\text{OCO})$ , whose dynamic dipole moments are polarized along the direction of the C-C bond. The absence of infrared activity from any of the other modes, especially  $\nu_{\text{as}}(\text{OCO})$ , would then suggest that acetate adopts a vertical, symmetric bidentate configuration. By analogy with the corresponding formate species on  $\text{Ag}\{111\}$ ,<sup>32</sup> we propose that acetate bridges two adjacent Ag atoms. Unlike formate, however, which tilts and forms three different monodentate species at high coverages,<sup>32</sup> acetate maintains an upright bidentate configuration at all surface coverages. This is probably due to the steric bulk of the methyl group which inhibits tilting.

Acetate species on other metal surfaces also appear to favor the same vertical, symmetric bidentate bridging mode. Similar arguments to those discussed above have been used to interpret the RAIR spectrum of acetate on  $\text{Ni}\{100\}$ ,<sup>8</sup> as well as the HREEL spectra of acetate on  $\text{Pt}\{111\}$ ,<sup>9</sup>  $\text{Pd}\{111\}$ ,<sup>10</sup>  $\text{Cu}\{111\}$ ,<sup>18</sup> and  $\text{Cu}\{100\}$ .<sup>28</sup> These conclusions are further supported by molecular orbital calculations for acetate on  $\text{Cu}\{100\}$ <sup>33</sup> and  $\text{Rh}_4$  clusters,<sup>34</sup> photoemission studies of acetate on  $\text{Cu}\{110\}$ ,<sup>35</sup> as well recent photoelectron diffraction studies of acetate on  $\text{Cu}\{110\}$ <sup>36</sup> and  $\text{Cu}\{100\}$ .<sup>33</sup>

**2. Polymerization of Acetaldehyde on Preoxidized  $\text{Ag}\{111\}$ .** Polyacetaldehyde is believed to exist in the form of spiral chains<sup>37</sup> while paraldehyde has a puckered ring form that matches the chair configuration of cyclohexane.<sup>38,39</sup> Their

(32) Sim, W. S.; Gardner, P.; King, D. A. *J. Phys. Chem.* **1996**, *100*, 12509.

(33) Sambì, M.; Granozzi, G.; Casarin, M.; Rizzi, G. A.; Vittadini, A.; Caputi, L. S.; Chiarello, G. *Surf. Sci.* **1994**, *315*, 309.

(34) Papai, I.; Ushio, J.; Salahub, D. R. *Surf. Sci.* **1993**, *282*, 262.

(35) Bao, S.; Liu, G.; Woodruff, D. P. *Surf. Sci.* **1988**, *203*, 89.

(36) Weiss, K. U.; Dippel, R.; Schindler, K. M.; Gardner, P.; Fritzsche, V.; Bradshaw, A. M.; Kilcoyne, A. L. D.; Woodruff, D. P. *Phys. Rev. Lett.* **1992**, *69*, 3196.

(37) Novak, A.; Whalley, E. *Can. J. Chem.* **1959**, *37*, 1710.

(38) Craven, E. C.; Jowitt, H.; Ward, W. R. *J. Appl. Chem.* **1962**, *12*, 526.

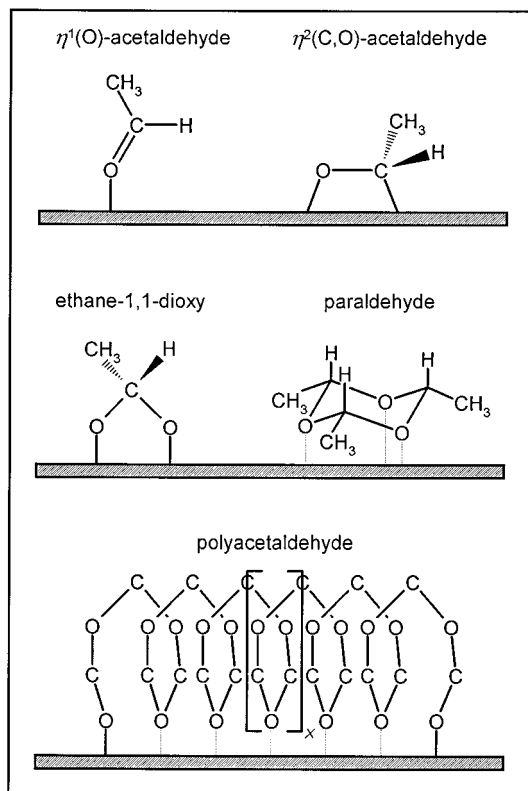
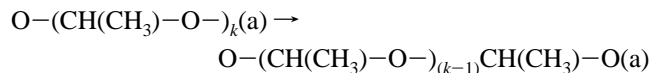
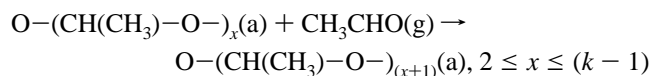
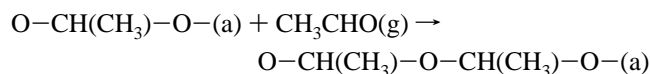
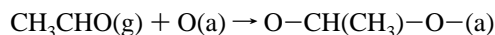


**Figure 4.** Structures of the possible species formed by the interaction of acetaldehyde with metal surfaces (Note: the CH<sub>3</sub> and H groups of polyacetaldehyde have been omitted for clarity).

structures and probable bonding modes to surfaces are depicted in Figure 4. Both compounds contain the common structural block ethane-1,1-dioxy, and as such their infrared spectra turn out to be very similar. This makes it somewhat difficult for us to attribute the RAIR spectra resulting from the low-temperature adsorption of acetaldehyde on preoxidized Ag{111}, which show matching absorption bands, to any one particular acetal species with absolute certainty based on their absorption frequencies alone. We can, however, rule out the possibility of  $\eta^1(\text{O})$ - and  $\eta^2(\text{C,O})$ -acetaldehyde (also illustrated in Figure 4) as these species have much higher C—O stretching frequencies that lie at 1600–1700 and 1300–1400  $\text{cm}^{-1}$ , respectively.<sup>16–18</sup> Single ethane-1,1-dioxy units would be expected to show a subset of the infrared absorption frequencies of polyacetaldehyde and paraldehyde. However, they are unlikely candidates for the low-temperature RAIR spectra as they cannot account for the observed band splittings. More importantly, their bidentate bonding configuration on the surface would be inconsistent with the appearance of the dipole-active  $\nu_{\text{as}}(\text{OCO})$  bands at 1160–1190  $\text{cm}^{-1}$ . An analogous situation has been reported for the HREEL spectra of formaldehyde adsorbed on preoxidized Ag{110} at 100 K,<sup>40</sup> which is consistent with both the infrared spectra of paraformaldehyde ((HCHO)<sub>n</sub>) chains and cyclic 1,3,5-trioxane ((HCHO)<sub>3</sub>).

Thermal desorption studies of acetaldehyde<sup>3</sup> and formaldehyde<sup>41</sup> adsorption on preoxidized Ag{110} indicate that an average of three and six aldehyde molecules, respectively, are adsorbed for each surface O atom present, although this does not necessarily imply that all the O becomes part of the adsorbed species initially formed. More importantly, the associated <sup>18</sup>O isotope labeling studies show that surface atomic O is incor-

porated into both the resultant carboxylate species and unreacted aldehydes.<sup>3,41</sup> This together with the inertness of clean Ag toward aldehydes<sup>3,41</sup> and the known nucleophilicity of surface atomic O<sup>42</sup> strongly suggests that the latter initiates coupling between aldehyde molecules by direct addition to the aldehyde C=O group so as to form a surface-bound dioxy fragment whose free O end (represented in the equations below by the O— atom with the dangling bond) can further add to another aldehyde molecule.<sup>40</sup> The process can be repeated such that more aldehyde molecules undergo sequential nucleophilic addition by the free O end (also represented in the equations below by the O— atom with the dangling bond) of the propagating oligomer.<sup>40</sup> A similar mechanism has been proposed for the bulk anionic polymerization of acetaldehyde which yields highly stereoregular macromolecular chains.<sup>43,44</sup> Since O atoms constitute both ends of the growing polymer, the most facile termination step would be bond formation with the surface to yield a chain structure:



It would be more difficult to envisage ring formation by elimination of the initiating O atom, given that it is expected to be a poor leaving group in such reactions. Moreover, aldehyde cyclization is known to be catalyzed by acids<sup>45</sup> rather than bases.

We thus believe that polyacetaldehyde is more likely to be present in this case, in agreement with the assignment of paraformaldehyde on Ag{110}.<sup>40</sup> Our RAIR spectra resemble closely the HREEL spectra of acetaldehyde adsorbed on preoxidized Cu{111},<sup>18</sup> where polyacetaldehyde has been identified. Acetaldehyde polymerization has also been reported on Ru{001}.<sup>17</sup> However, the absorption bands in this case do not agree so well with bulk polyacetaldehyde, and could alternatively be assigned to  $\eta^2(\text{C,O})$ -acetaldehyde and acetyl species, as was observed on Pd{111}.<sup>16</sup> Formaldehyde polymerization on metal surfaces induced by the clean surface, coadsorbates, or even photons, is much more widespread, and paraformaldehyde species with very similar HREEL spectra have been observed on Ag{111},<sup>46</sup> Ag{110},<sup>40</sup> Cu{110},<sup>47</sup> Ni{110},<sup>48</sup> Rh{111},<sup>49</sup> Pd{111},<sup>16</sup> Pt{111},<sup>50</sup> and Fe{100}.<sup>51</sup>

### 3. Structure of Polyacetaldehyde on Preoxidized Ag{111}. From X-ray diffraction studies of crystalline polyacetaldehyde<sup>52</sup>

- (41) Barteau, M. A.; Bowker, M.; Madix, R. J. *Surf. Sci.* **1980**, *94*, 303.
- (42) Madix, R. J. *Science* **1986**, *233*, 1159.
- (43) Vogl, O. *J. Polym. Sci. A* **1964**, *2*, 4607.
- (44) Vogl, O. *J. Polym. Sci. A* **1964**, *2*, 4633.
- (45) Bevington, J. C. *Q. Rev., Chem. Soc.* **1952**, *6*, 141.
- (46) Fleck, L. E.; Ying, Z. C.; Dai, H. L. *J. Vac. Sci. Technol. A* **1993**, *11*, 1942.
- (47) Sexton, B. A.; Hughes, A. E.; Avery, N. R. *Surf. Sci.* **1985**, *155*, 366.
- (48) Richter, L. J.; Ho, W. *J. Chem. Phys.* **1985**, *83*, 2165.
- (49) Houtman, C.; Barteau, M. A. *Surf. Sci.* **1991**, *248*, 57.
- (50) Henderson, M. A.; Mitchell, G. E.; White, J. M. *Surf. Sci.* **1987**, *188*, 206.
- (51) Hung, W. H.; Bernasek, S. L. *Surf. Sci.* **1996**, *346*, 165.
- (52) Natta, G.; Mazzanti, G.; Corradini, P.; Bassi, I. W. *Makromol. Chem.* **1960**, *37*, 156.

(39) Boero, J. F. R.; de Mandirola, O. B. *J. Chim. Phys. Phys.-Chim. Biol.* **1976**, *73*, 163.

(40) Stuve, E. M.; Madix, R. J.; Sexton, B. A. *Surf. Sci.* **1982**, *119*, 279.

and paraformaldehyde<sup>53–55</sup> it has been concluded that the polymer C–O backbones assume a helical chain configuration. This has been further confirmed by ab initio calculations<sup>56,57</sup> and AFM studies<sup>58</sup> of paraformaldehyde. Infrared spectra of polyacetaldehyde<sup>37,59</sup> and paraformaldehyde<sup>60–63</sup> have also been shown to be consistent with this structure. Provided that the interchain interactions are weak, which is usually the case, the spectra may be interpreted in terms of that of a hypothetical isolated helical chain containing  $n$  monomer units with  $m$  turns and belonging to the one-dimensional space group  $C(2m\pi/n)$ .<sup>61,64</sup> This means that each HCHO or CH<sub>3</sub>CHO monomer unit in the chain can be transformed into a neighboring one by a rotation of  $2m\pi/n$  and a translation by a factor of  $1/n$  the unit cell length along the chain axis, where  $m$  and  $n$  are integers. For any arbitrary  $m$ , one can make use of the symmetry properties of the isomorphous point group  $C_n$  to show that the infrared-active vibrations belong to the symmetry species A and E<sub>1</sub> (B for  $n = 2$  and E for  $n = 3$  or 4) with dynamic dipole moments polarized parallel and perpendicular to the chain, respectively.<sup>61,64</sup> Since the infrared activities of the polymer vibrations are independent of the value of  $n$ , these conclusions should be valid for both paraformaldehyde and polyacetaldehyde with any general helical structure of symmetry  $C(2m\pi/n)$ . Crystalline polyacetaldehyde chains possess  $C(\pi/2)$  symmetry,<sup>52</sup> while the two crystalline forms of paraformaldehyde that have been found have a higher symmetry ( $D(10\pi/9)$ <sup>53,54</sup> and  $D(\pi)$ <sup>55</sup>). However, except for the A modes splitting into infrared-inactive A<sub>1</sub> species and infrared-active A<sub>2</sub> species, the selection rules for the general case of a helical chain with  $D(2m\pi/n)$  symmetry are identical to that in the  $C(2m\pi/n)$  situation.

Therefore, for the general case of  $C(2m\pi/n)$  symmetry, each vibration of the monomer unit essentially gives rise to three infrared-active modes (A + E<sub>1</sub>) of the polymer, while the translations and rotations together contribute to another fourteen (4A + 5E<sub>1</sub>). For the free polymer chain both components of each E<sub>1</sub> mode are degenerate and give rise to a single absorption band. However, this degeneracy can be removed if the polymer is bound to a solid surface such that the symmetry is reduced to C<sub>1</sub>. This is precisely the case for the adsorbed polyacetaldehyde and paraformaldehyde, which are expected to interact with the surface through the O lone pairs and hence lie with their chain axes oriented roughly parallel to the surface. By the metal–surface selection rule, the original A modes would then have their dynamic dipole moments along the surface and become infrared-inactive while the infrared activities of the originally E<sub>1</sub> modes will depend on the rotational orientation of the polymer skeletal backbone about the chain axis. We thus believe that all the observed features in the RAIR spectra of polyacetaldehyde on Ag{111} arise from what were originally the E<sub>1</sub> modes, and the lifted degeneracy is responsible for the splitting of several of the bands. Many previous reports of polyacetaldehyde and paraformaldehyde on metal surfaces have

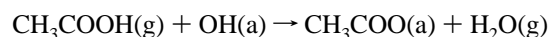
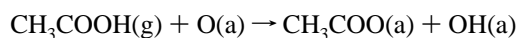
depicted them as having planar zigzag skeletal backbones consisting of alternating C and surface-bound O atoms.<sup>17,18,40,47,50,51</sup> This picture is misleading as it disagrees with the known helical structure of these polymers, and is at odds with the observed surface vibrational spectra. The  $\nu_{\text{as}}(\text{OCO})$  vibration of the planar zigzag C–O chain would give rise to a dynamic dipole moment directed along the chain axis and hence parallel to the surface, which should be screened according to the metal–surface selection rule. Yet this mode is dipole active for adsorbed polyacetaldehyde<sup>17,18</sup> and becomes particularly strong for adsorbed paraformaldehyde.<sup>16,40,46–51</sup> On the other hand, the observed surface vibrational spectra are entirely consistent with spiral polymer chains lying along the surface as at least one element (from the original E<sub>1</sub> mode) of the  $\nu_{\text{as}}(\text{OCO})$  vibration will then possess some component of its dynamic dipole moment normal to the surface and thus show infrared activity.

The helical polymer configuration is not the only structure that could account for our RAIR spectra, and there may be other possible polymer configurations, where not all the O atoms of the polymer lie in a common plane parallel to the surface, which could give rise to infrared-active  $\nu_{\text{s}}(\text{OCO})$  and  $\nu_{\text{as}}(\text{OCO})$  vibrations. However, given the overwhelming evidence for the helical structure of crystalline polyacetaldehyde and paraformaldehyde, and the weak perturbation that Ag surfaces are known to exert on most adsorbates,<sup>42</sup> we anticipate that polyacetaldehyde should retain its helical structure when adsorbed on Ag{111}. Ab initio calculations have also shown that helical paraformaldehyde adsorbed on a metal surface (in this case a cluster model of the Al{100} surface) should be a stable entity.<sup>57</sup>

In the bulk state, helical polyacetaldehyde chains with  $C(\pi/2)$  symmetry crystallize in the tetragonal form, yielding a spiral pitch of 4.8 Å.<sup>52</sup> For paraformaldehyde, the  $D(10\pi/9)$  and  $D(\pi)$  forms exist as hexagonal and orthorhombic crystals respectively with spiral pitches of  $\sim 3.5$  Å.<sup>53–55</sup> The interatomic distance for most transition metals is between 2.5 and 2.9 Å. It can be envisaged that the adsorbed polyaldehyde chains, which form two-dimensional structures on the surface, would have some degree of conformational mobility not available in the bulk crystalline state which allows them to maximize their bonding interactions with the surface. This may be brought about by changing the spiral pitch to match the surface registry and forming helices that increase the interaction of the O and metal atoms by reducing the steric hindrance of the attached H and methyl groups. An example structure of polyacetaldehyde with  $C(2\pi/3)$  symmetry and (and more exposed O atoms as compared to the  $C(\pi/2)$  structure) is shown adsorbed on Ag{111} in Figure 4, although it is not possible at this stage to deduce the true conformation based on the vibrational spectra alone.

The unavoidable close approach of some of the attached H and methyl groups to the metal surface might be expected to influence the subsequent decomposition pathways of adsorbed polyacetaldehyde and paraformaldehyde. However, it appears that in virtually all cases, the polymers tend to depolymerize via C–O bond scission before the metal surface can induce any significant C–H bond activation.<sup>16–18,21,22,40,46–51</sup> As such, there does not appear to be any correlation between the polymer stability and metal identity.

**4. Formation of Acetate on Ag{111}.** The reaction of acetic acid with surface atomic O to produce acetate, OH, and H<sub>2</sub>O is a classic acid–base reaction, where the H<sub>2</sub>O formed desorbs during the dose for surface temperatures above 200 K:<sup>4</sup>



(53) Tadokoro, H.; Yasumoto, T.; Murahashi, S.; Nitta, I. *J. Polym. Sci.* **1960**, *44*, 266.

(54) Uchida, T.; Tadokoro, H. *J. Polym. Sci. A2* **1967**, *5*, 63.

(55) Carazzolo, G.; Mammi, M. *J. Polym. Sci. A* **1963**, *1*, 965.

(56) Karpfen, A.; Beyler, A. *J. Comput. Chem.* **1984**, *5*, 19.

(57) Seel, M.; Kunz, A. B.; Wadiak, D. T. *Phys. Rev. B* **1988**, *37*, 8915.

(58) Snetivy, D.; Yang, H. F.; Glomm, B.; Vancso, G. J. *J. Mater. Chem.* **1994**, *4*, 55.

(59) Furukawa, J.; Saegusa, T.; Fujii, H.; Kawasaki, A.; Imai, H.; Fujii, Y. *Makromol. Chem.* **1960**, *36*, 149.

(60) Philpotts, A. R.; Evans, D. O.; Sheppard, N. *Trans. Faraday Soc.* **1951**, *55*, 1051.

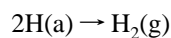
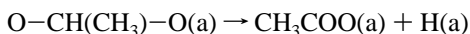
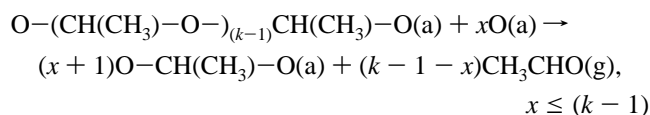
(61) Novak, A.; Whalley, E. *Trans. Faraday Soc.* **1959**, *55*, 1484.

(62) Tadokoro, H.; Kobayashi, M.; Kawaguchi, Y.; Kobayashi, A.; Murahashi, S. *J. Chem. Phys.* **1963**, *38*, 703.

(63) Zamboni, V.; Zerbi, G. *J. Polym. Sci. C* **1964**, *7*, 153.

(64) Tadokoro, H. *J. Chem. Phys.* **1960**, *33*, 1558.

The generation of acetate from acetaldehyde reaction with surface atomic O at 140 K starts with polyacetaldehyde formation as described previously. On heating we observe first a reorientation of the polymer chains by rotation about their axes, as indicated by the disappearance of one component of each doublet. This is accompanied by an increase in the intensity of  $\nu_s(\text{OCO})$  relative to  $\nu_{as}(\text{OCO})$ , possibly due to heat- and O-induced breakdown of the polymer into free acetaldehyde that desorbs and ethane-1,1-dioxy fragments that are essentially upright bidentate species where  $\nu_{as}(\text{OCO})$  is infrared-inactive. The ethane-1,1-dioxy then decomposes by elimination of H to yield acetate. It appears from the RAIR spectra that all the intermediates coexist on the surface between 140 and 180 K:



The desorption of acetaldehyde and  $\text{H}_2$  occurred at 220–250 K on Ag{110}, and was also proposed to originate from ethane-1,1-dioxy dehydrogenation to acetate.<sup>3</sup> We have found a similar sharp  $\text{H}_2$  desorption peak at  $\sim 230$  K. An analogous mechanism has been put forward for formaldehyde decomposition on preoxidized Ag{110} based on HREELS<sup>40</sup> and thermal desorption studies,<sup>41</sup> where it was suggested that the polymer linkage inhibits the dehydrogenation of the dioxy species to formate.

The surface acetate species on Ag{111} is stable up to  $\sim 450$  K, above which it decomposes into products that we have been unable to detect. These would be expected to be the same as for acetate decomposition on Ag{110} in the absence of surface atomic O, namely  $\text{CO}$ ,  $\text{CO}_2$ ,  $\text{H}_2$ ,  $\text{H}_2\text{O}$ , and ketene.<sup>3,4</sup>

## 5. Conclusions

We have studied the reaction of acetic acid and acetaldehyde with surface atomic O on Ag{111}. The surface acetate species is formed in both cases, and based on the symmetry and dynamic dipole moments of its normal modes of vibration, we conclude that acetate adopts a vertical, bidentate bridging configuration. No coverage dependence of the adsorption geometry was observed. While acetic acid undergoes direct deprotonation by O to produce acetate at 240 K, acetaldehyde is subject to nucleophilic attack by O that initiates polymerization into polyacetaldehyde at 140 K. By a detailed symmetry analysis we have shown that the RAIR spectra of polyacetaldehyde on Ag{111}, as well as HREEL spectra of polyacetaldehyde and paraformaldehyde on other metal surfaces, are most consistent with the polymer chains adopting helical configurations and bonding to the surface through O atoms at various points along their skeletal backbones. On heating, polyacetaldehyde breaks down into free acetaldehyde and surface-bound ethane-1,1-dioxy units, which dehydrogenate completely by 220 K to yield acetate.

**Acknowledgment.** We thank the EPSRC for an equipment grant and a postdoctoral assistantship (P.G.). One of us (W.S.S.) acknowledges a scholarship from the Cambridge Commonwealth Trust and St. John's College, Cambridge.

JA960662H